Catalysis Today 157 (2010) 77–82

Contents lists available at ScienceDirect

Catalysis Today

journal homepage: www.elsevier.com/locate/cattod

# Preparation of Au–Pd/C catalysts by adsorption of metallic species in aqueous phase for selective oxidation

Sophie Hermans*, Aurore Deffernez, Michel Devillers

*Institut IMCN, Université catholique de Louvain, 1/3 Place Louis Pasteur, B-1348 Louvain-la-Neuve, Belgium*

ARTICLE INFO

*Article history:*
Available online 13 May 2010

*Keywords:*
Adsorption
Selective oxidation
Heterogeneous catalysis
Carbon
Palladium
Gold

ABSTRACT

Au/C and Au–Pd/C catalysts were prepared on SX PLUS activated carbon using an adsorption method in which the precursor(s)–support interactions in aqueous solution were sought to be optimized. pH windows where maximum adsorption occurs were identified for four bimetallic cases, varying the incorporation order of the adsorbed metallic precursors and the oxidation state of the first metal introduced. All samples were characterized by XPS and SEM/EDXS, and the above-mentioned parameters were found to have an influence on the surface microstructure of the samples and on the activity of the bimetallic catalysts obtained. This preparation method leads to highly active catalysts for the selective oxidation of glucose, with the activity correlated with high surface Pd/C ratios.

## 1. Introduction

Gold-based catalysts have proven important for environmental and fine chemicals applications [1]. Supported gold catalysts are active in a variety of reactions, including in liquid phase [2]. Three main groups have demonstrated the activity of carbon-supported Au to oxidize alcohols [3–5], carbohydrates [6,7] and aldehydes [8]. These recent developments have led researchers to investigate the effect of adding other metals to gold within supported catalysts. Combinations of gold with platinum group metals have displayed potential for industrial applications, and in particular Pd–Au catalysts supported on carbon for liquid phase oxidations [9,10].

It is known that the activity of supported catalysts depends on the size and distribution of the metal particles, which depends on the preparative method and the support [11]. Many techniques allow the preparation of highly dispersed gold catalysts, such as using precursors containing Au and the support metal component, favoring strong support–Au interactions, using pre-formed colloidal Au. However, most of these do not use carbon as support and are not suitable for bimetallic materials. In addition, acidic, neutral and/or basic surface groups (due to hetero-atoms, mainly O, N and S) present on the surface of activated carbon influence its surface characteristics and adsorption behavior [12]. Consequently, charged surface sites exist in aqueous phase, depending on the pH, and relying amongst other things on the point of zero charge (PZC). Below that value the carbon surface is positively charged, while above that value the surface is negatively charged, attracting ions with the opposite charge. This implies an electrostatic mechanism of adsorption. This concept was used by Regalbuto and co-workers [13] to obtain highly dispersed and highly loaded Pt/carbon materials. We believe that it is important to go one step further and to study also the influence of the metallic species charge present in solution on their adsorption behavior.

In this paper, our goal is to maximize the interactions between the metallic precursor(s) and the activated carbon support in aqueous solution, by studying the adsorption of Au and Pd species on activated carbon SX PLUS in order to prepare Au(5 wt.%)–Pd(5 wt.%)/C catalysts. To do so, adsorption curves for Au and Pd on C were established in order to identify the pH windows where a maximal amount of metal adsorbs. The influence of the incorporation order of the two metallic precursors and the oxidation state of the first metal introduced when adsorbing the second one were also studied. In order to test the simple electrostatic view to explain the maximum adsorption windows, the respective charges of the support surface and of the metallic species in solution were determined. The metal speciation in solution was calculated from the stability constants of the various compounds involving the $H_2O$, $OH^-$ and/or $Cl^-$ ligands. Finally, the Au–Pd samples (prepared within the identified optimal adsorption windows) were reduced to bimetallic Au–Pd/C catalysts and tested in glucose selective oxidation in comparison with their monometallic analogues.

## 2. Experimental

### 2.1. Starting materials

An SX PLUS activated carbon supplied by NORIT (abbreviated as C in this paper, $S_{BET} \approx 900\,m^2\,g^{-1}$, particle size = 50–100 μm, total

---

* Corresponding author. Tel.: +32 10 472810; fax: +32 10 472330.
*E-mail address:* Sophie.Hermans@uclouvain.be (S. Hermans).

0920-5861/$ – see front matter © 2010 Elsevier B.V. All rights reserved.
doi:10.1016/j.cattod.2010.04.010

acidity = 32.0 mmol/100 g) was used as support. The metal precursors were $Pd(OAc)_2$ (Aldrich, 98%) and $HAuCl_4·3H_2O$ (Aldrich, 99.9+%).

### 2.2. Preparation of starting monometallic Pd and Au samples

Two carbon-supported Pd samples (activated and non-activated) and one activated Au/C sample containing 5 wt.% of metal were prepared, based on earlier studies [12,14]. The first Pd sample was prepared by impregnation (24 h contact time) in aqueous solution at pH 4 from $Pd(OAc)_2$ solubilized with nitric acid and is noted $Pd(OAc)_2/C$. The second Pd sample was prepared similarly but with an additional reduction step by formalin at pH 10 (1 h at 80 °C), and is simply named Pd/C. The Au/C sample was prepared by impregnation (24 h) in aqueous solution of $HAuCl_4$ at pH 10, and reduction by formalin at 80 °C (pH 10, 1 h).

### 2.3. Determination of supports surface charge

The point of zero charge (PZC) was determined by a modified literature method [15], by bringing 1 g of solid sample in contact with 10 mL of water at a fixed pH, and measuring the resulting pH after 24 h. This operation is repeated over a range of initial pH values (3–12), and the PZC corresponds to the plateau obtained when plotting the measured pH versus the initial fixed pH.

### 2.4. Establishment of adsorption curves

The general procedure is to bring into contact a sample of support suspended in water with a solution of metal precursor for 24 h and then to determine the amount of non-adsorbed metal in the filtrate, and to repeat this for a range of pH values. The pH was fixed by the addition of $Na_2CO_3$, NaOH or $HNO_3$. The monometallic cases were described previously [12,14]. For the bimetallic Au–Pd samples (noted $M_2 - M_1/C$ where $M_1$ is the first metal introduced), the influence of the two metal precursors incorporation order and of the oxidation state of the first metal introduced were studied. Four bimetallic adsorption curves were established. When the starting monometallic sample was not reduced before incorporating the second metal, the experimental procedure consisted in the following: an aqueous solution of given first metal concentration (calculated by considering a monolayer of metallic precursor molecules on the SX PLUS carbon surface and neglecting the area developed by the micropores [12], i.e. 0.025 g of $HAuCl_4·3H_2O$ or 0.056 g of $Pd(OAc)_2$ solubilized with nitric acid) at fixed pH was added to an aqueous suspension of 0.238 g carbon pre-conditioned at the same pH value in order to get a final volume of 100 mL and the suspension was agitated for 24 h. Then, 50 mL of a solution containing the second metal precursor pre-conditioned at the same pH value was added and stirred for an additional 24 h before filtration. Depending on the incorporation order, the two adsorption curves obtained between pH 1 and 14 will be called $Pd(OAc)_2$–$HAuCl_4/C$ and $HAuCl_4$–$Pd(OAc)_2/C$. If a reduction step of the first metal ($M_1$) was added, the second metallic precursor (0.05 g of $HAuCl_4·3H_2O$ or 0.053 g of $Pd(OAc)_2$) was solubilized in 50 mL water before being stabilized at a given pH and transferred to an aqueous suspension of 0.238 g monometallic sample (reduced Pd(5 wt.%)/C or Au(5 wt.%)/C) pre-conditioned at the same pH value and the mixture was stirred during 24 h before filtration. Again, depending on the incorporation order, these two bimetallic cases will be named $Pd(OAc)_2$–Au/C and $HAuCl_4$–Pd/C. The adsorption filtrates containing the non-adsorbed Pd and/or Au were analyzed by atomic absorption spectrometry, and the amount of metals adsorbed on the support at each different pH value was deduced by subtraction. In this study, we call "adsorption samples" all the solids recovered by filtration at the end of the adsorption experiments.

### 2.5. Control experiments

In order to check the possibility of bulk precipitation, control experiments were carried out at ambient temperature as follows, using the highest concentration used for the preparations, without support. 50 mg of $Pd(OAc)_2$ was solubilized in 2 mL concentrated $HNO_3$. Then 50 mL of water was added and the solution stirred until complete dissolution. Solid $Na_2CO_3$ was added cautiously in order to increase the pH. This experiment was repeated in order to obtain solutions at various fixed pH. The solutions were left to stand for 24 h before observation.

### 2.6. Physico-chemical characterization techniques

X-ray photoelectron spectroscopy (XPS) was performed on an SSI-X-probe (SSX-100/206) spectrometer from Fisons. The samples were stuck onto troughs with double-sided adhesive tape, then placed on an insulating home-made ceramic carrousel with a nickel grid 3 mm above the samples, to avoid differential charging effects. A floodgun set at 8 eV was used for charge stabilization. The energy scale was calibrated by taking the Au $4f_{7/2}$ binding energy at 84 eV. The $C_{1s}$ binding energy of contamination carbon set at 284.8 eV was used as internal standard value. Data treatment was performed with the CasaXPS program (Casa Software Ltd). The analyses of palladium and gold were based on the Pd3d and Au4f photopeaks and the following constraints were used for decomposition: intensity ratios $I(\text{Pd } 3d_{5/2})/I(\text{Pd } 3d_{3/2}) = 1.5$ and $I(\text{Au } 4f_{7/2})/I(\text{Au } 4f_{5/2}) = 1.33$, FWHM ratios = 1, $\Delta(\text{Pd } 3d_{5/2} - \text{Pd } 3d_{3/2}) = 5.26$ eV and $\Delta(\text{Au } 4f_{7/2} - \text{Au } 4f_{5/2}) = 3.67$ eV. Scanning Electron Microscopy (SEM) analyses were performed on a field effect gun Digitan Scanning Electron Microscope (DSM 982 Gemini from LEO), equipped with an energy dispersive X-ray system (EDAX Phoenix equipped with a CDU LEAP detector). The powder samples were pressed onto conducting double-face adhesive tape fixed onto 0.5″ aluminum specimen stubs from Agar Scientific. The quantification of Pd and Au in solution was made by atomic absorption analysis, using a Perkin-Elmer 3110 spectrometer equipped with an air–acetylene flame atomizer. Calibration curves (from 1 to 10 mg/L for Pd and from 1 to 15 mg/L for Au) were realized with standard solutions obtained by dilution of commercial palladium (1006 μg/mL, Acros) and gold (1003 μg/mL, Aldrich) solutions.

### 2.7. Catalysis

Bimetallic catalysts and their monometallic analogues were synthesized by impregnation in aqueous solution, using the pH values where maximum adsorption occurs, and maintaining it throughout all synthetic steps. The procedure is similar to the establishment of the adsorption curves, with an additional step consisting in activating in situ the catalysts with formalin or $NaBH_4$. Catalytic tests were performed in a thermostatised double-walled glass reactor equipped with an automatic titration device for pH control, as described previously [12,14]. The materials were compared, in the oxidation of glucose, on the basis of the yield in gluconic acid (only detected secondary product is fructose).

## 3. Results and discussion: adsorption curves

### 3.1. Determination of support surface charge

The PZC value obtained for C was 8.5 [12]. Two other PZC values were determined: (i) after adsorption of Pd acetate on C (sample named $Pd(OAc)_2/C$) and (ii) after its reduction, giving sample

**Table 1**
XPS results for monometallic $Pd(OAc)_2/C$, Pd/C [12] and Au/C samples.

| Sample (M = Pd, Au) | M/C (×100)[a] | |
|---|---|---|
| | Calc. | Exp. |
| $Pd(OAc)_2/C$ | 0.6 | 13.1 |
| Pd/C | 0.6 | 4.0 |
| Au/C | 0.3 | 0.86 |

[a] M/C atomic intensity ratios: calc. = values calculated from the bulk composition in the case of 100% adsorption and without taking into account the carbon contribution of the ligands, exp. = experimental values retrieved from XPS data analysis.

named Pd/C: values of 4.7 and 9.6 were obtained, respectively. In the first case, the presence of remaining acetates, and the fact that the sample was prepared at pH 4, might explain the obtained acidic value. In the second case, the fact that the Pd/C sample presents a PZC value superior to the PZC value of C could be explained by the reduction by formalin of some of the surface acidic functions during the activation step.

### 3.2. Characterization of starting monometallic Pd and Au samples

Samples Pd/C [12], $Pd(OAc)_2/C$ and Au/C were characterized by XPS and SEM (Table 1 and Fig. 1). The Pd/C surface atomic ratios measured for the two Pd samples are very high (0.04 and 0.13) in comparison with the value calculated on the basis of the bulk composition (0.006), suggesting a high concentration of palladium on the surface, probably in a relatively dispersed form. In opposite, the Au/C surface ratio of the Au/C sample (0.0086) is more similar to the calculated value (0.003), meaning that either gold penetrates more in the porous network or is present as larger aggregates. This was visualized by electron microscopy. The SEM images of the $Pd(OAc)_2/C$ sample (Fig. 1a) show a precipitate of Pd covering the carbon surface while the electron micrographs of the Pd/C sample (Fig. 1b) show a homogeneous distribution of relatively small Pd particles (~10–15 nm in size). This might explain the huge difference of Pd/C ratios measured by XPS (respectively, 0.13 and 0.04), as the precipitate must be mainly located at the external surface while the quite smaller particles might have penetrated the porous network more hence be less detected by XPS. The SEM images of the Au/C sample (Fig. 1c) reveal an agglomeration of metallic particles on the carbon surface, with particles sizes up to 200 nm. In all three cases, the microstructure obtained is far from ideal, as far as particles sizes are concerned, especially in the case of gold, where obtaining small particles is known to be crucial for the catalytic activity.

When studying the adsorption of Au on C, it was observed that the whole amount of metal introduced in solution was adsorbed on the support over the whole pH range [14]. The XPS Au/C surface ratios were weak, with a maximum value of 0.012 at pH 9 [14]. The distribution of Au(III) species in solution was determined from the stability constants [16,17]: all gold species envisaged ($Cl^-$ and $OH^-$ ligands) were negatively charged [14]. This explains the absence of clear maximum in the Au/C adsorption curve. The weak Au/C ratios determined by XPS could be related to the agglomeration of Au in the form of big particles. This might be explained by the concept of *aurophilicity* [18,19], which favors the close packing of adsorbed gold ions. Moreover, the reducing nature of carbon limits the deposition of gold in a dispersed state, as observed for Au/C catalysts prepared by deposition–precipitation [18]. This last effect must be the most important, as reduction of gold by the surface must occur readily and give the observed big particles.

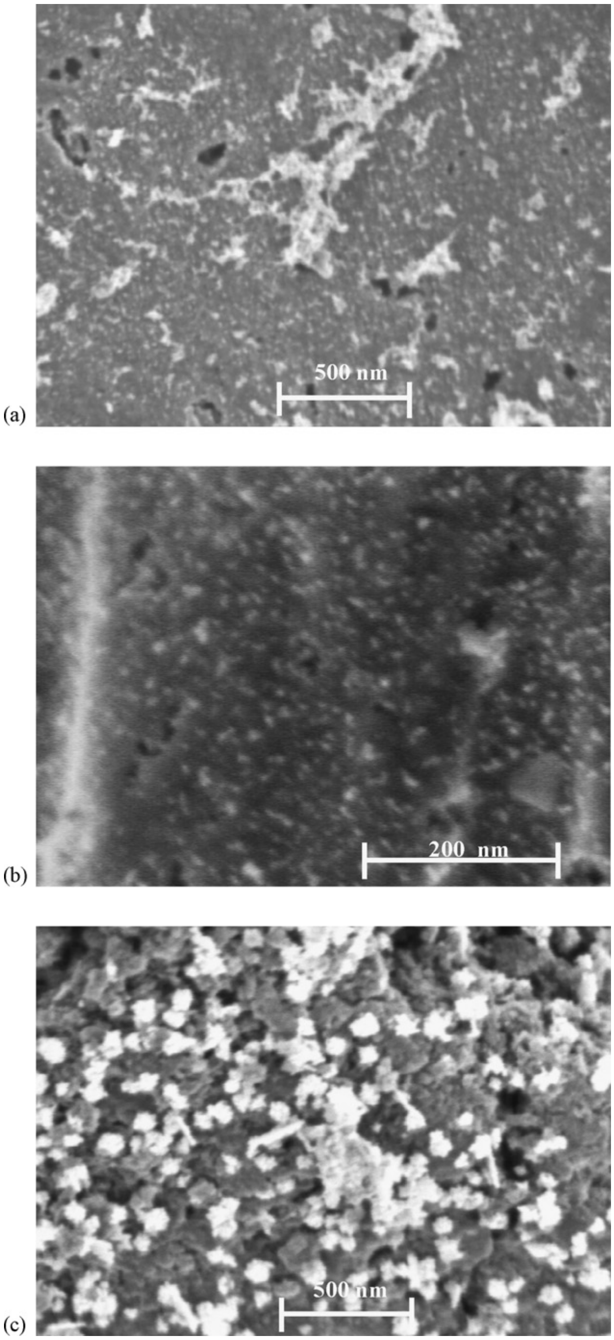

**Fig. 1.** SEM images obtained for starting monometallic samples: (a) $Pd(OAc)_2/C$ (50 000×), (b) Pd/C (200 000×) [12], (c) Au/C (50 000×).

**Table 2**
Summary of observations for bimetallic adsorption samples.

| Sample | Support PZC | Maximum adsorption | Optimum (highest M/C XPS ratios) | SEM |
|---|---|---|---|---|
| $Pd(OAc)_2$–Au/C | 8.5 (C) | pH 3–12 | pH 5 | Big particles |
| $Pd(OAc)_2$–$HAuCl_4$/C | 8.5 (C) | pH 3–12 | pH 10 | Pd precipitates + big Au particles (>200 nm) |
| $HAuCl_4$–$Pd(OAc)_2$/C | 4.7 ($Pd(OAc)_2/C$) | pH 1–9 | pH 9 | Pd precipitates + big Au particles (>200 nm) |
| $HAuCl_4$–Pd/C | 9.6 (Pd/C) | pH 1–9 | None | Small Pd particles (<10 nm) + big Au particles (>50 nm) |

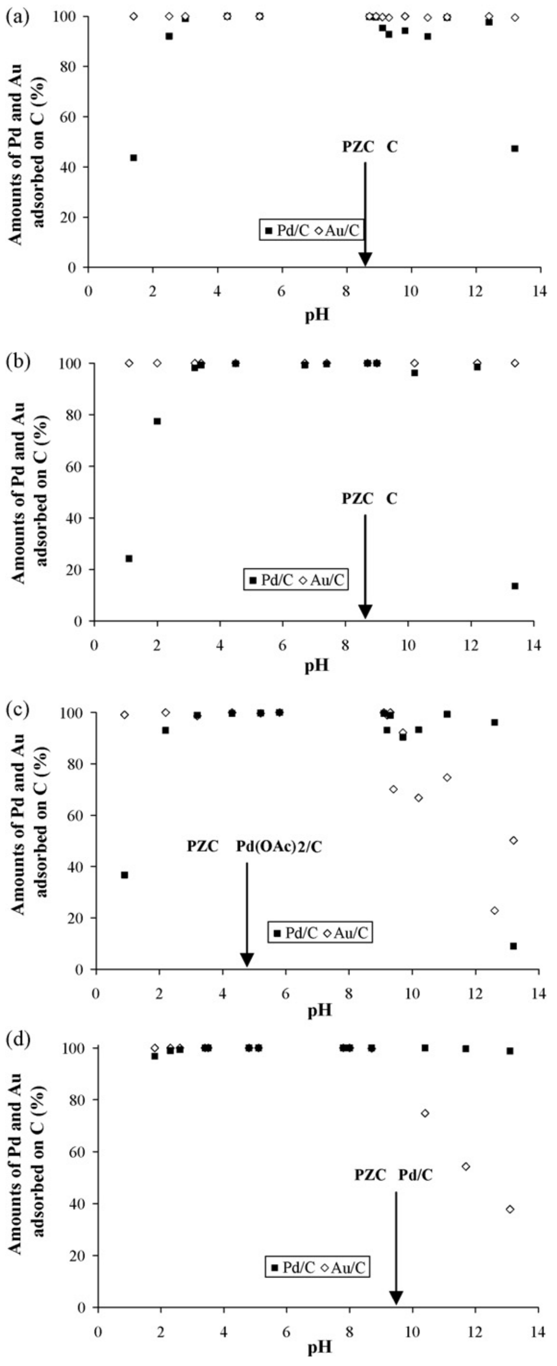

**Fig. 2.** Bimetallic adsorption curves in aqueous phase: (a) $Pd(OAc)_2$–Au/C, (b) $Pd(OAc)_2$–$HAuCl_4$/C, (c) $HAuCl_4$–$Pd(OAc)_2$/C, (d) $HAuCl_4$–Pd/C, (■) amount of Pd adsorbed on C, (◇) amount of Au adsorbed on C.

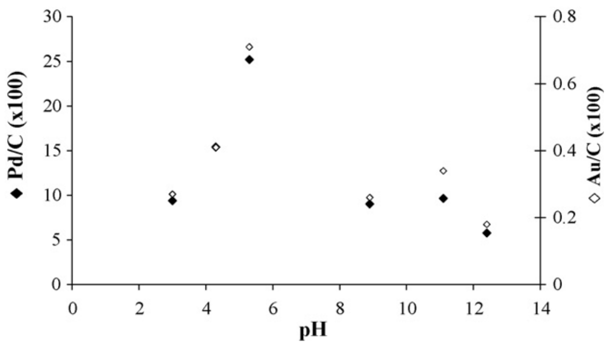

**Fig. 3.** Pd/C and Au/C surface ratios determined by XPS for bimetallic adsorption samples: $Pd(OAc)_2$–Au/C, as representative example.

### 3.3. Bimetallic adsorption curves

Four bimetallic adsorption curves have been determined, differentiated by the incorporation order and the oxidation state of the first metal adsorbed (Table 2). The adsorption curve named $Pd(OAc)_2$–Au/C gives a maximum adsorption window between pH 3 and 12 for Pd, and reveals that no leaching of Au occurs (Fig. 2a). This pH range is identical for the adsorption curve $Pd(OAc)_2$–$HAuCl_4$/C (Fig. 2b). By opposition, the window of Au adsorption is reduced between pH 1 and 9 when introducing the Pd precursor first ($HAuCl_4$–$Pd(OAc)_2$/C, Fig. 2c). Finally, adsorbing the Au precursor on a Pd(5 wt.%)/C sample gives a total adsorption of Au at pH below 9, while no Pd leaching is observed ($HAuCl_4$–Pd/C, Fig. 2d).

Some solid samples arising from each bimetallic adsorption curve have been characterized by XPS. The results obtained with the $Pd(OAc)_2$–Au/C samples are illustrated as an example in Fig. 3. The first three adsorption curves reveal pH values where the Pd/C and Au/C atomic intensity ratios are maximum: at pH 5, 10 and 9 for the $Pd(OAc)_2$–Au/C, $Pd(OAc)_2$–$HAuCl_4$/C and $HAuCl_4$–$Pd(OAc)_2$/C curves, respectively. The adsorption curve giving the highest Pd/C ratios (between 0.058 and 0.252), in comparison with the calculated value (0.0125) on the basis of the bulk composition in the case of 100% adsorption, is $Pd(OAc)_2$–Au/C. In opposite, it is the $HAuCl_4$–$Pd(OAc)_2$/C curve which gives the highest Au/C ratios (up to 0.018) when compared with the calculated value (0.0028). The analysis by XPS of the fourth case ($HAuCl_4$–Pd/C) did not give a pH range where Pd/C and Au/C ratios were optimized, and the absolute values of Pd/C ratios were much smaller.

The adsorption samples arising from the first three curves and giving the highest Pd/C and Au/C ratios by XPS have been examined by SEM/EDXS. The images of the sample prepared at pH 5 in the case of the $Pd(OAc)_2$–Au/C curve (Fig. 4a) show big particles (>100 nm) and the EDXS analysis gives the signals corresponding to carbon and gold. In the two other cases ($Pd(OAc)_2$–$HAuCl_4$/C and $HAuCl_4$–$Pd(OAc)_2$/C), SEM analysis of, respectively, the samples prepared at pH 10 and 9 revealed precipitates of Pd and big particles of Au (>200 nm) covering the carbon surface (Fig. 4b and c). EDXS analyses within the microscope confirmed the nature of each type of particle observed. The difference between these two cases is the density of Pd precipitate, which is higher when Pd is introduced first. We have also analyzed by SEM/EDXS (Fig. 5) two adsorption samples (prepared at pH 5 and pH 10) belonging to the fourth adsorption curve ($HAuCl_4$–Pd/C). No major difference between these two samples was observed. Detailed examination of the images shows a distribution of small Pd particles (<10 nm) and big Au particles (>50 nm) in the two cases.

In order to determine whether an electrostatic adsorption model can be invoked, the distribution of Pd and Au species in solution was determined from stability constants [16,17,20] using the experimental conditions (pCl = 2.77) used for establishment of the two adsorption curves without reduction. Fig. 6 shows the speciation diagram for Pd(II): neutral $[Pd(OH)_2(H_2O)_2]$ is the major species for pH 4–12. Au speciation is identical to the distribution obtained previously [14]: Au species are negatively charged over the whole pH range. Thus, the metals charge in solution does not explain why we do not obtain the same trend for the two bimetallic curves without reduction: if the Au precursor is introduced first, the total amount of gold remains adsorbed at all pH values, while if the Pd precursor is incorporated first, the maximum adsorption window of gold is reduced (pH < 9). The surface of the $Pd(OAc)_2$/C sample is negatively charged at pH superior to 4.7 as evidenced by PZC determination.

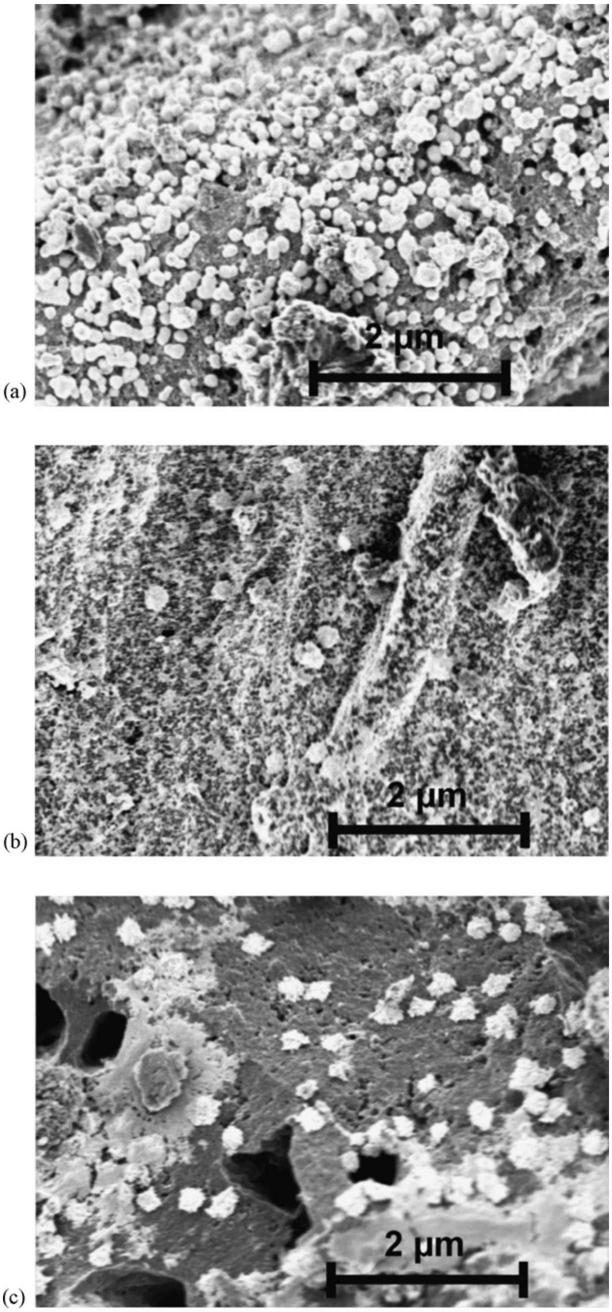

**Fig. 4.** SEM images obtained for the bimetallic samples adsorbed at optimized pH: (a) $Pd(OAc)_2$–Au/C at pH 5 (20 000×), (b) $Pd(OAc)_2$–$HAuCl_4$/C at pH 10 (20 000×), (c) $HAuCl_4$–$Pd(OAc)_2$/C at pH 9 (20 000×).

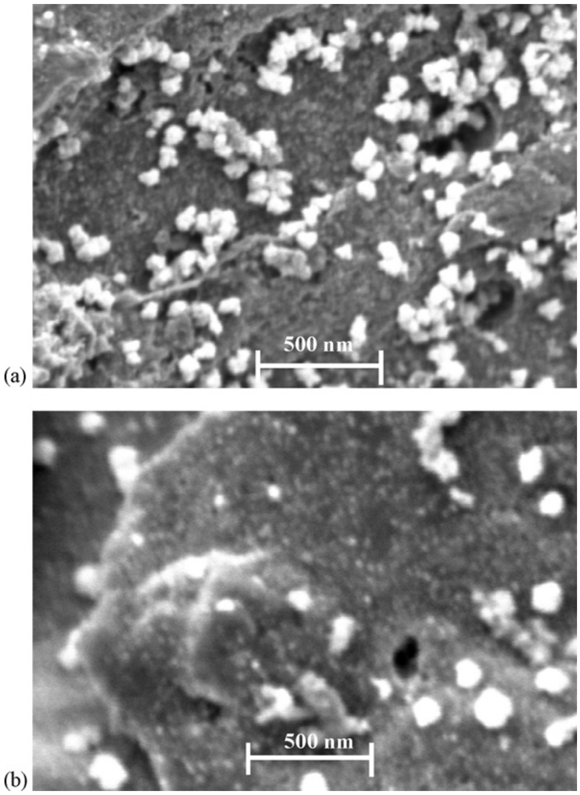

**Fig. 5.** SEM images obtained for the bimetallic samples $HAuCl_4$–Pd/C prepared: (a) at pH 5 (50 000×), (b) at pH 10 (100 000×).

When the Pd precursor is introduced first and if we consider that its major form is the neutral complex $[Pd(OH)_2(H_2O)_2]$, the charge state of the support is not modified but the available surface area for the adsorption of gold has decreased (if one considers that gold would preferably sit on the bare support rather than on palladium). So, the adsorption of gold at pH superior to the PZC value is not favored due to the identical charge of the support and Au metallic species, and due to the lower available surface area. The $HAuCl_4$–Pd/C adsorption curve could be explained similarly: the charge of the Pd/C surface and the Au species are both negative at pH superior to 9.6, and the Au adsorption is reduced in this pH window. By opposition, the adsorption of the acidic gold precursor in first position could decrease the PZC value of the support. However, the presence of Au has no effect on the amount of Pd adsorbed. Characterization by SEM/EDXS of the bimetallic samples giving the best Pd/C and Au/C XPS ratios showed that the incorporation order also had an influence on the surface microstructure. Gold is present as big particles (Au + C detected by EDXS) while Pd displays better dispersed smaller particles (undetectable by EDXS), but these particle sizes are far from ideal. It appears that an electrostatic mechanism does not allow the windows of maximum adsorption to be explained. A deposition–precipitation process within the window where neutral species are present must be invoked. Control experiments were carried out, by preparing a range of Pd solutions at various fixed pH (between 1 and 14), by dissolving $Pd(OAc)_2$ at the highest concentration used in the preparation. These solutions were left to stand without support for 24 h and homogeneous bulk precipitation indeed occurred. This precipitation phenomenon might be slow in dilute solutions without support but is accelerated by the presence of the support in suspension. This also means that speciation data calculated from a restricted set of equilibrium

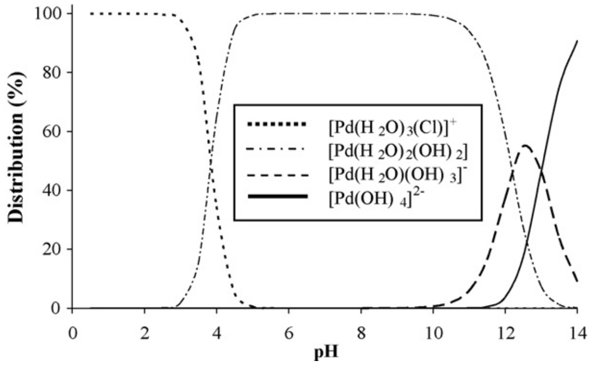

**Fig. 6.** Distribution of Pd(II) species as a function of pH: $H_2O$, $Cl^-$ and $OH^-$ as ligands, pCl = 2.77.

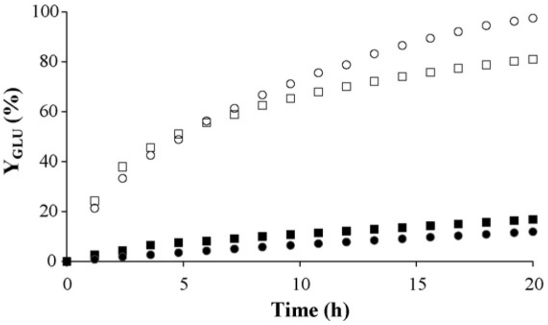

**Fig. 7.** Comparison of catalytic results for Pd(5 wt.%)/C and Au(5 wt.%)–Pd(5 wt.%)/C materials in glucose oxidation: (■) $Pd(OAc)_2$/C activated with formalin, (●) $Pd(OAc)_2$/C activated with $NaBH_4$, (□) $HAuCl_4$–$Pd(OAc)_2$/C activated with formalin, (○) $HAuCl_4$–$Pd(OAc)_2$/C activated with $NaBH_4$.

constants based on hypothetical Pd species are not accurate, and even more when considering the preparation of heterogeneous catalysts as the solid supports interferes in the kinetics for some species formation. Precipitation on the surface of the support would result in irregular aggregates and big particles. This phenomenon explains the large windows of adsorption, the discrepancy between surface and metallic species charges when adsorption occurs, the SEM images showing precipitates and the irregular XPS ratios. In the case of gold, self-reduction in solution, or when contacting the carbon surface, must also be considered. These two events would participate in the growth of big particles at the surface.

## 4. Preliminary catalytic results

Bimetallic catalysts were prepared by impregnation in aqueous solution by keeping the pH in the maximum adsorption windows, followed by chemical activation. The Au–Pd/C catalysts prepared here give performances superior to their Pd/C and Au/C (totally inactive) monometallic analogues (Fig. 7), demonstrating the synergetic effect between these two metals. The optimization of the synthetic conditions allowed the preparation of catalysts which are active and selective, even if the particles are big, especially in the case of gold. Thus the present synthetic method is not competitive regarding particles sizes but gives results in terms of performance. The bimetallic catalysts described here give similar results than with the most performant Bi(5 wt.%)–Pd(5 wt.%)/C catalysts for glucose oxidation [21] (sample Ac·PdBi/$C_{SX+}$ prepared by deposition of carboxylate precursors on the same carbon SX PLUS giving $Y_{GLU}/m_{Pd}$ ($t = 4$ h) = 17.52% $mg^{-1}$ or sample noted ref·PdBi/$C_{SX+}$ prepared by a patented procedure giving $Y_{GLU}/m_{Pd}$ ($t = 4$ h) = 21.48% $mg^{-1}$ to compare with $Y_{GLU}/m_{Pd}$ ($t = 4$ h) = ∼9.5% $mg^{-1}$ with Pd–Au/C samples here). In the same testing conditions [21], a commercial trimetallic Pd–Pt–Bi/C catalyst from Degussa gave $Y_{GLU}/m_{Pd}$ ($t = 4$ h) = 19.2% $mg^{-1}$. However, the Bi-based formulation suffered from a major drawback that is overcome here: leaching of promoter element in solution.

The obtained Au–Pd/C catalysts present weak Au/C and relatively high Pd/C surface ratios (measured by XPS) and metallic Pd on the surface, suggesting a relatively good dispersion of Pd on the support. The catalysts presenting the highest Pd/C ratios give the best catalytic activity in glucose selective oxidation. These observations suggest that high activities are related to high Pd surface concentration and to an efficient reduction into Pd metal. In addition, SEM/EDXS characterization indicates that the least active catalysts display separated small Pd particles and big Au particles, while the more active materials reveal either a homogeneous distribution of smaller Pd and Au particles, or a precipitate covering the carbon surface. The surface structure of these bimetallic materials influences thus their catalytic activity. It implies that the incorporation order of the two metals and the oxidation state of the first metal introduced influence both the structure and the performance of the catalysts. Only metallic gold was detected in all catalysts by powder XRD. This observation can be related to the relative sizes of Au and Pd particles, which as described above, are very big in the case of gold and relatively small in the case of Pd. The bimetallic material activated with $NaBH_4$, showing the highest Pd/C and Au/C ratios and a precipitate covering the carbon surface, is the most active in the oxidation of glucose into gluconic acid.

## 5. Conclusion

This work aimed at studying the adsorption of Au and Pd precursor(s) on activated carbon in aqueous phase. Adsorption curves were realized to identify maximum adsorption windows, followed by characterization of the adsorption samples. The results of four bimetallic adsorption curves were slightly different: the precursors' incorporation order influences the amount of metal adsorbed on the support and the microstructure of the samples obtained. The presence of Pd on the support has an effect on the amount of Au adsorbed, while the presence of Au does not seem to influence the quantity of adsorbed Pd. SEM images of the sample presenting the highest XPS Pd/C and Au/C ratios revealed a Pd precipitate in contact with big Au particles. The results allowed to discard a simple electrostatic model because the maximum adsorption ranges correspond to the existence of neutral Pd species and negative Au species, while the support is either positively or negatively charged but were consistent with a surface deposition–precipitation process. The Au–Pd/C catalysts prepared by this method are very active in glucose oxidation, and more so than their monometallic analogues, indicating a synergetic effect between the two metals. They are characterized by high Pd/C surface ratios and relatively small metallic Pd particles. The metals incorporation order and oxidation state as well as the activating agent used also influence the catalytic performance.

## Acknowledgments

The authors acknowledge financial support from the FNRS and the Belgian State (Belgian Science Policy, IAP Project INANOMAT No. P6/17), NORIT for supplying carbon SX PLUS, E.M. Gaigneaux, M. Genet, and J.-F. Statsijns for discussions and technical assistance.

## References

[1] M. Haruta, Gold Bull. 37 (2004) 27–36.
[2] L. Prati, G. Martra, Gold Bull. 32 (1999) 96–101.
[3] L. Prati, F. Porta, Appl. Catal. A 291 (2005) 199–203.
[4] S. Demirel, P. Kern, M. Lucas, P. Claus, Catal. Today 122 (2007) 292–300.
[5] G.J. Hutchings, Gold Bull. 37 (2004) 3–11.
[6] Y. Onal, S. Schimpf, P. Claus, J. Catal. 223 (2004) 122–133.
[7] M. Comotti, C. La Pina, R. Matarrese, M. Rossi, A. Siani, Appl. Catal. A 291 (2005) 204–209.
[8] S. Biella, L. Prati, M. Rossi, J. Mol. Catal. A: Chem. 197 (2003) 207–212.
[9] N. Dimitratos, A. Villa, D. Wang, F. Porta, D.S. Su, L. Prati, J. Catal. 244 (2006) 113–121.
[10] L. Prati, A. Villa, F. Porta, D. Wang, D.S. Su, Catal. Today 122 (2007) 386–390.
[11] M. Haruta, Catal. Today 36 (1997) 153–166.
[12] A. Deffernez, S. Hermans, M. Devillers, J. Phys. Chem. C 111 (2007) 9448–9459.
[13] X. Hao, L. Quach, J. Korah, W.A. Spieker, J.R. Regalbuto, J. Mol. Catal. A: Chem. 219 (2004) 97–107.
[14] A. Deffernez, S. Hermans, M. Devillers, Stud. Surf. Sci. Catal. 162 (2006) 79–86.
[15] J. Park, J.R. Regalbuto, J. Colloid Interface Sci. 175 (1995) 239–252.
[16] L.G. Sillen, Stability Constants of Metal–Ion Complexes: Section I, The Chemical Society, London, 1964.
[17] S.A. Wood, Geochim. Cosmochim. Acta 55 (1991) 1759–1767.
[18] G.C. Bond, C. Louis, D.T. Thompson, Catalysis by Gold, Imperial College Press, London, 2006.
[19] H. Schmidbaur, A. Schier, Chem. Soc. Rev. 37 (2008) 1931–1951.
[20] I.V. Mironov, L.D. Tsvelodub, Russ. J. Inorg. Chem. 45 (2000) 633–637.
[21] M. Wenkin, R. Touillaux, P. Ruiz, B. Delmon, M. Devillers, Appl. Catal. A 148 (1996) 181.